
Ensemble learning-based classification on local patches from magnetic resonance images to detect iron depositions in the brain

Beshiba Wilson*

Department of CSE,
Noorul Islam Centre for Higher Education,
Tamil Nadu, India
Email: beshibaw@gmail.com
*Corresponding author

Julia Punitha Malar Dhas

Noorul Islam Centre for Higher Education,
Tamil Nadu 629180, India
Email: julaps113@yahoo.com

Ruma Madhu Sreedharan

Government Medical College,
Kollam, Kerala 691574, India
Email: rumamadhu@yahoo.com

Ram P. Krish

VisionCog Research and Development Private Limited,
Civil Station Road, Peroorkada,
Thiruvananthapuram 695005, Kerala, India
Email: ram.krish@visioncog.com

Abstract: Iron deposition in the brain has been observed with normal aging and is associated with neurodegenerative diseases. The automated classification of brain magnetic resonance images (MRI) based on iron deposition in Basal Ganglia region of the brain has not been performed, to our knowledge. It is very difficult to analyse iron regions in brain using simple MRI techniques. The MRI sequence namely susceptibility weighted imaging (SWI) helps to distinguish brain iron regions. The objective of our work is to investigate the iron regions in selected areas of basal ganglia region of brain and classify MR images. The study included a total of 60 MRI images which consists of 40 subjects with iron region and 20 subjects of healthy controls. We performed Gaussian smoothing followed by construction of 40 localised patches of each MR image based on iron and normal regions. Grey level co-occurrence matrix (GLCM) features are extracted from the patches and fed to random forest (RF) classifier for patch-based classification of iron region. Training of data patch features was done by random forest classifier and the performance of classifier in terms of accuracy was measured. The experimental results show that the proposed localised patch-based approach for classification of brain iron images using random forest classifier achieved 96.25% classification accuracy in identifying normal and iron regions from brain MR sequences.

Keywords: ensemble learning; classification; iron deposition; magnetic resonance images; MRI; susceptibility weighted images; SWI; grey level co-occurrence matrix; GLCM; random forest classifier; RF classifier; neurodegenerative diseases; basal ganglia; Gaussian smoothing.

Reference to this paper should be made as follows: Wilson, B., Dhas, J.P.M., Sreedharan, R.M. and Krish, R.P. (2021) 'Ensemble learning-based classification on local patches from magnetic resonance images to detect iron depositions in the brain', *Int. J. Bio-Inspired Computation*, Vol. 17, No. 4, pp.260–266.

Biographical notes: Beshiba Wilson started her career in teaching since December 2003. She is presently the Head of the Department of Computer Science and Engineering, Lourdes Matha College of Science and Technology, Kerala, India. She is an MTech graduate in Computer Science and Engineering. She is currently pursuing research in the field of machine learning and medical imaging. She has taught a variety of computer courses including neural networks, computer graphics, python programming, image processing, soft computing, fuzzy logic and

microcontrollers. She has worked in many diverse areas such as machine learning, neural networks, medical image processing and computer graphics. She has published more than 15 papers in various international journals and conferences. She is a life member of Indian Society for Technical Education (ISTE) and faculty member of Computer Society of India (CSI). She won the Best Paper Award in the International Conference on Novel Issues and, Challenges in Science and Engineering'16 (NICSE'16).

Julia Punitha Malar Dhas has a vast experience in teaching and currently the Professor and Deputy Director (Research) in Noorul Islam Centre for Higher Education, Tamil Nadu. Her areas of interests are mainly computer networks and image processing. She has published many papers in international journals and conferences.

Ruma Madhu Sreedharan is a radiologist and works as an additional Professor in Radiodiagnosis in Government Medical College, Kollam, Kerala, India. She has published many papers related to medical imaging. Her research interests include susceptibility weighted imaging and diffusion tensor imaging.

Ram P. Krish received his PhD in Computer Science and Telecommunication Engineering from Universidad Autónoma de Madrid, Spain, and pursued his postdoctoral research work at Dublin City University, Ireland. His doctoral and postdoctoral research works were funded by the prestigious European Commission's Marie Curie Fellowship. He was also a visiting researcher at University of Twente, Netherlands and University of Halmstad, Sweden. He graduated from Chennai Mathematical Institute, India. He is currently the Founder and Director of VisionCog Research & Development Private Limited, India. His research interests and area of expertise includes computer vision, machine learning, deep learning, biometrics, and algorithm development.

1 Introduction

Iron is deposited in the form of hemosiderin in many regions of brain which leads to human cognitive ageing (Valdes Hernandez et al., 2015). Neurodegeneration with accumulation of brain iron leads to neurodegenerative diseases (Kruer et al., 2012). Increased quantity of iron in brain has been related to chronic brain disorders like Alzheimer's disease, movement disorders particularly Parkinson's disease and dystonia, multiple sclerosis, cognitive dysfunction, retinal abnormalities and other disorders (Hosseini Sadrzadeh and Saffari, 2004; Stankiewicz et al., 2007; Araujo Salomao et al., 2016). Excessive iron in the brain results in oxidative stress and neuronal dysfunction as well as death (Batista-Nascimento et al., 2012). Schipper (2012) relates seven disorders of neurodegeneration with brain iron accumulation (NBIA) with strong emphasis on neuroimaging. Gregory and Hayflick (2004) suggest that NBIA targets various types of disorders related to neurodegeneration diseases. Neuroferritinopathy is a neurodegenerative disorder which is related to brain iron accumulation. The actual cause of Neuroferritinopathy is mutation in ferritin light chain gene (Ohta and Takiyama, 2012).

Thomas et al. (1993) found that there is age-related deposition of iron in five regions of brain (substantia nigra, putamen, red nucleus, dentate nucleus and caudate) from T2-weighted MRI spin-echo images. Magnetic resonance imaging (MRI) studies shows that in most forms of NBIA, the iron deposition mainly occurs in the crucial brain

regions of basal ganglia (Kruer and Boddaert, 2012) such as globus pallidus (Kruer, 2013), putamen and caudate (Yan et al., 2012). Lanciego et al. (2012) has shown that globus pallidus, putamen and caudate are categorised under basal ganglia and related nuclei. Susceptibility weighted imaging (SWI) is a neuroimaging technique in which the differences in magnetic susceptibility of tissues are used in the enhancement of contrast of MRI (Haacke et al., 2009, 2004). Sheelakumari et al. (2017) has performed a quantitative analysis of iron content in the MR sequence namely SWI. The work reveals a potential biomarker for frontotemporal dementia. The identification of iron content in brain facilitates efforts to provide treatments for the associated neurodegenerative diseases.

In the proposed work, a new local patch-based approach is introduced to perform feature extraction in the brain SWI sequences. Ensemble learning techniques are used to identify and classify the iron regions in brain.

2 Related works

Recently, the quantification of iron in MRI brain images is a hot research point. The identification and classification of iron content in brain using automated techniques is not yet fully developed. A survey on various stages involved in the automated detection and classification of brain tumour areas namely feature extraction, segmentation and classification is discussed in this section.

2.1 Feature extraction

A prominent attribute of an image is the texture of an image. Udayabhanu et al. (2016) suggests that the statistical method of examining the textures is grey level co-occurrence matrix (GLCM) and it considers spatial relationship between the pixels.

2.2 Segmentation

Vijay et al. (2016) has proposed the enhanced Darwinian particle swarm optimisation (EDPSO) technique for identification and segmentation of regions of tumour in MRI. EDPSO particles find an optimal solution in search space by computing the best neighbourhood.

2.3 Classification

Zacharakia et al. (2006) introduces a recursive feature elimination (RFE) approach in support vector machine (SVM) to determine a subset of attributes using backward sequential selection method and optimises the performance of the classifier. Zhang et al. (2015) has proposed an automated classification method based on eigenbrains and SVM technique to detect Alzheimer's disease related brain regions in 3D MR images.

3 Dataset

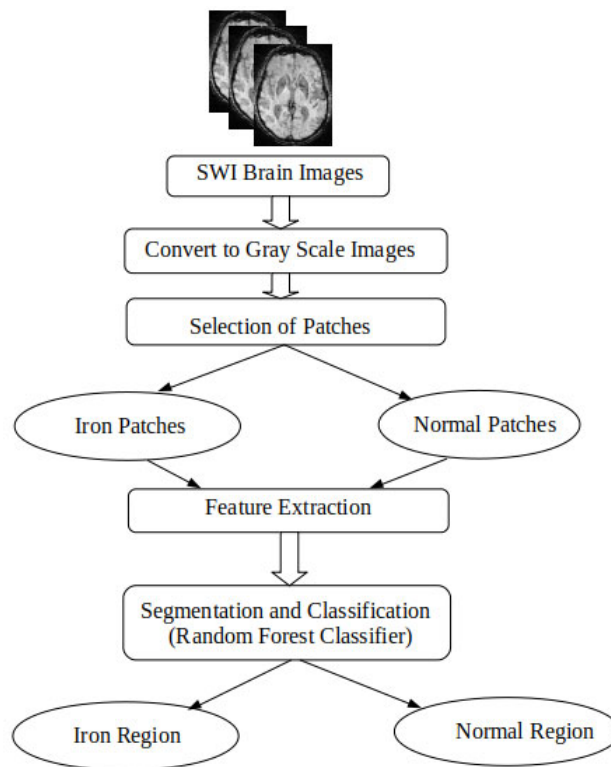
OASIS-3 dataset (Oasis Brains Datasets, <http://www.oasis-brains.org>.) is used for the implementation of the proposed work. The slices include axial view of susceptibility weighted images of 3.0 Tesla MR Sessions obtained using Siemens TIM Trio 3T MRI Scanner. The brain image subjects includes 60 cases both men and women aged 60 to 80 with 40 iron subjects and 20 healthy controls. The iron regions in three main parts of basal ganglia namely globus pallidus, putamen and caudate were analysed in this study. Finally, the iron regions in each image were outlined with the help of experienced radiologist. The outlined images are considered to be the ground truth. All experiments were conducted using Scikit Learn version 0.20 and Scikit Image version 0.14.1 under Python version 3.6.7.

4 Proposed work

Figure 1 illustrates the steps of our proposed work.

The proposed work for identification and classification of iron regions in brain comprises of the fundamental stages such as region of interest (ROI) selection, construction of local patches, and extraction of features and classification. We propose a novel patch-based approach using robust classification techniques to identify and classify iron regions in brain MRI.

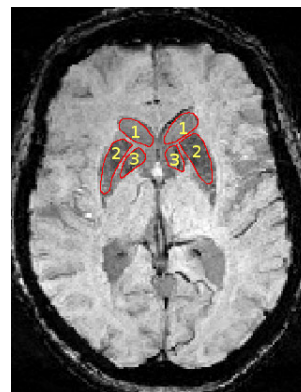
Figure 1 Flowchart of the proposed work



4.1 ROI selection

The regions of interest of brain MRI include three main parts of basal ganglia namely globus pallidus, putamen and caudate. The SWI image slices showing these regions are selected for image manipulations. All the original images are available in RGB format. Initially, the RGB images are converted into grey scale images. SWI Images are usually prone to Gaussian and Rician noise. The Gaussian smoothing is performed on the grey scale image by applying Gaussian function which filters the noise in the image. The iron content in the three regions under consideration is analysed with the help of an expert radiologist and the images are considered to be the ground truth. Figure 2 shows the main parts of basal ganglia used in this work.

Figure 2 Manual selection of ROI – (1) caudate, (2) putamen and (3) globus pallidus regions of basal ganglia in SWI brain image (see online version for colours)



4.2 Construction of local patches

Based on the ROI, iron regions and normal regions in the selected parts of basal ganglia are identified. For each subject, 20 core pixels each from iron and normal regions are extracted. A 21×21 patch is constructed for the selected 20 pixels of iron region and 20 pixels of normal region. From Figure 3, it is clear that most of the nearby patches overlap with each other. From the selected pixels, a total of 40 patches are constructed which includes 20 patches for iron regions and 20 patches for normal regions for each image as shown in Figures 4 and 5. The 21×21 patches are constructed with the identified core pixel as the centre of a given image patch. For iron classification from brain SWI, the iron pixels are recognised from the localisation of the central pixel in a particular patch. These localised patches combined with feature extraction techniques are used to train the classifier.

Figure 3 Axial view of SWI image showing 21×21 patches for selected iron and normal regions in brain image (see online version for colours)

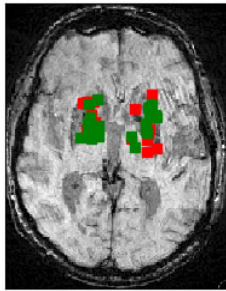


Figure 4 Enlarged view of 21×21 patches of iron regions (1 to 20 patches)

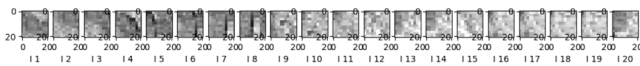
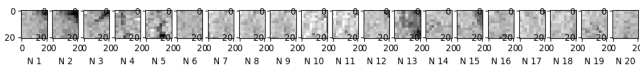


Figure 5 Enlarged view of 21×21 patches of normal regions (1 to 20 patches)



4.3 Extraction of features

The feature extraction is performed based on GLCM. The GLCM features namely dissimilarity, correlation, contrast, homogeneity, angular second moment (ASM) and energy are extracted from the localised patches of iron and normal regions.

The statistical analysis of texture in brain images comprises of determining the patch-based features from the intensity variations in iron regions and normal regions. Thus a total of 240 image features are extracted from 40 patches based on the six GLCM features for each image.

The number of rows and columns in the matrix determine the size of the GLCM matrix. The variations in intensity levels (i and j) at distance d for an angle θ are

deployed for the calculation of GLCM features (Haralick et al., 1993; Wilson and Dhas, 2016).

a Dissimilarity

The dissimilarity weights increases linearly from the diagonal and is represented as,

$$DS = \sum_{i,j=0}^{GL-1} G_{i,j}(i-j) \quad (1)$$

b Correlation

The correlation of an image is the measure of linear dependency of grey levels of the pixel positions. It is represented as,

$$CR = \sum_{i=0}^{GL-1} \sum_{j=0}^{GL-1} \frac{\{i \times j\} \times G(i,j) - \{\mu_x \times \mu_y\}}{\sigma_x \times \sigma_y} \quad (2)$$

c Contrast

The local intensity variation is the measure of contrast which increases with weight values. The diagonal values on GLCM show no contrast, and contrast increases away from GLCM diagonal values.

$$Contrast = \sum_{i,j=0}^{GL-1} G_{i,j}(i-j)^2 \quad (3)$$

d Homogeneity or inverse difference moment (IDM)

The homogeneity has a greater impact on the IDM. The weight associated with homogeneity is influenced by regions which are inhomogeneous. This results in a low IDM value for images which are not homogeneous and high value for other images.

$$Homogeneity = \sum_{i=0}^{GL-1} \sum_{j=0}^{GL-1} (1/1+(i-j)^2)G(i,j) \quad (4)$$

e Angular second moment

The estimation of homogeneity in an image is described by ASM. A homogeneous group of pixels consists of small number of grey levels, resulting in a GLCM with less grey levels but high values of $G(i,j)$. This implies that the sum of squares will be high.

$$ASM = \sum_{i=0}^{GL-1} \sum_{j=0}^{GL-1} \{G(i,j)\}^2 \quad (5)$$

f Energy

Energy is the texture measure obtained by determining the square root of the ASM values. It is represented as

$$E = \sum_{i=0}^{GL-1} \sum_{j=0}^{GL-1} (G(i,j))^2 \quad (6)$$

Discriminative textural features in local patches thus obtained are used for training the classifier.

4.4 Classification

The main role of machine learning includes classification problems and is widely used in many applications in the last few years. In our proposed system, the iron dependent features are determined using the local patch-based extraction of features. The features that are extracted are then trained using various classifiers in machine learning such as logistic regression (LR), linear SVM, kernel SVM (radial basis function), decision tree and ensemble learning-based random forest classifier.

a Logistic regression

LR (Perez Ortiz et al., 2016) is technique which is widely used in statistical modelling. In this technique, an approximation method is adopted by which the likelihood that an object 's' is in class 'X' is determined by considering one particular class as the pivot class.

b Linear SVM

Kotsiantis et al. (2006) introduces that SVM is one of the modern machine learning techniques based on supervised classification. In SVM, a margin is used to separate two classes of different patterns. The main aim of the SVM is to maximise the margin so as to increase the gap between the hyper planes (Perez Ortiz et al., 2016).

c Kernel SVM (radial basis function)

In the case of nonlinear boundaries, Kernel functions are used along with the SVMs (Perez Ortiz et al., 2016). A kernel function is related to a nonlinear mapping function. Main advantages of kernel SVM are that the computation of the model is simplified and it enables more accurate decision functions.

d Decision tree

Murthy (1998) and Kotsiantis et al. (2006) states that a decision tree is generated from a set of training objects. A set of attributes along with a class label describes each object in the training set. Based on feature values, the decision trees classify the instances. A feature is represented by a node in the decision tree and branch denotes a value of the node.

e Naive Bayes

Naive Bayes classifier (NBC) is amongst the most popular learning method grouped by similarities, which works on the popular Bayes' theorem of probability to build machine learning models particularly for disease prediction and document classification. The NBC-based classification includes two processes, i.e., the training process and the validation process. During the training process, the image subjects are categorised as normal and abnormal classes (Bustomi et al., 2018).

f Ensemble learning-based random forest classifier

Random forest classifier is a machine learning techniques which is widely applied in image

classification (Horning, 2010). In order to calculate the response, the results from several models are used in this ensemble model-based random forest. In random forest method, many decision trees are grown and the response is determined from the output of all the decision trees. During training process, the probabilities for each class at each leaf node are determined for each tree (Bosch et al., 2007). The efficiency of the random forests depends on how the decision trees are created to generate the forest.

5 Experimental results and discussion

To validate the performance of the proposed work, 60 MR images (slices of SWI axial view) of brain were used in our experiment. The manual segmentation was initially done by experts on the images which are considered to be the ground truth images. Better results were obtained by Gaussian smoothing images compared to the original grey scale image. Totally 240 features were obtained from the 20 iron patches and 20 normal patches for each image based on the six GLCM features. The influence of patch sizes 10×10 , 15×15 and 21×21 were also studied. Based on the analysis, optimal results were achieved for patch size 21×21 . The histogram analysis of the training data, i.e., GLCM features shows varying diversity of values. In addition to the six GLCM grey scale features extracted, six gradient features are extracted from the MR image by applying a discrete differentiation operator called the Sobel operator. This operator computes an approximation of the gradient of the image intensity function.

Based on both the extracted grey scale and gradient features, the values of α_g and α_p (weighted coefficients of grey scale and gradient operator respectively) were empirically computed by performing an exhaustive search using Grid search technique. The grid search is performed by assigning the values of α from 0.1 to 1 with a step size of 0.1 for determining optimal values of α_g and α_p . From the exhaustive search conducted through experiments, it is evident that the optimal value of $\alpha_g = 0.3$ and $\alpha_p = 0.7$. The proposed mathematical model for computation of discriminative features (both grey scale and gradient features) by assigning appropriate weight values is given below:

$$D(f_g, f_p) = \sum_{n=1}^N [\alpha_g \cdot f_g(n) + \alpha_p f_p(n)] \quad (7)$$

where weighted coefficients $\alpha_g = 0.3$ and $\alpha_p = 0.7$;

f_g grey scale features

f_p first order features obtained using Sobel operator

n represents the patch in the template patch library.

The analysis of optimal value for the weighted coefficients of grey scale and gradient features was performed using six state of the art machine learning classifiers. From Table 1, it is evident that the maximum value for classification

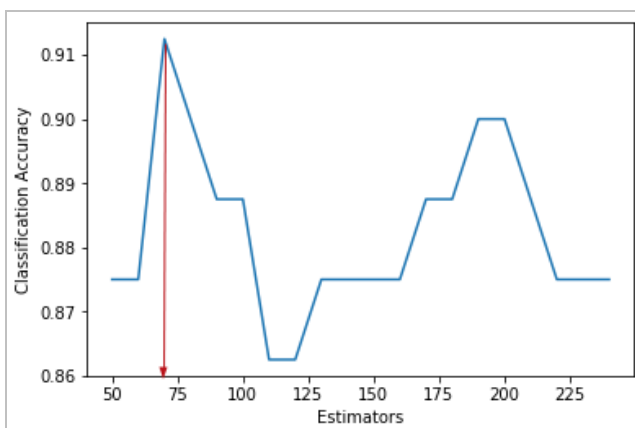
accuracy is obtained with $\alpha_g = 0.3$ and $\alpha_p = 0.7$. The peak value of classification accuracy is obtained for the proposed machine learning-based classification model.

Table 1 Comparison of classification accuracy of various machine learning methods based on the optimal values of α_g and α_p (weighted coefficients of grey scale and gradient operator respectively) computed using grid search technique

Method used	Classification accuracy		
	With	With	With
	$\alpha_g = 0.4$	$\alpha_g = 0.3$	$\alpha_g = 0.2$
	$\alpha_p = 0.6$	$\alpha_p = 0.7$	$\alpha_p = 0.8$
Logistic regression	57.25	66.87	62.50
Linear SVM	70.30	71.25	63.75
Kernel SVM (RBF)	81.67	75.62	76.25
Naive Bayes	83.15	88.75	85
Decision tree	86.25	93.15	91.35
Proposed RF	93.50	96.25	92.75

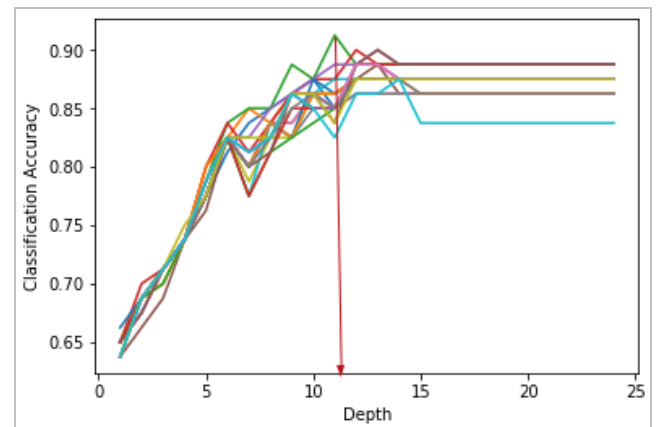
The ratio of test data to training data was fixed as 20:80. The classification accuracy is determined by using the mean accuracy on the given test data samples. The classification accuracy is the percentage of true predictions made divided by the entire number of predictions done. We found that random forest classifier outperforms all other classification methods. The influence of two important parameters of random forest classifier namely number of estimators and depth was also performed in this work. A search for the optimal estimator value of RF classifier gave significant results for score with the estimator value 71. The variation of estimators with classification accuracy is illustrated in Figure 6.

Figure 6 Classification accuracy vs. estimators for RF classifier (see online version for colours)



Similarly, a search for the optimal depth value of RF classifier showed that maximum classification accuracy was achieved with depth value 11. Thus the best classification score was achieved by the specified optimal depth value. The variations of depth with classification accuracy are shown in Figure 7.

Figure 7 Classification accuracy vs. depth values for RF classifier (see online version for colours)



6 Conclusions

The detection of iron region in NBIA is important for the evaluation and treatment of iron overload in various diseases related to neurodegeneration. A novel technique for extraction of features for identification and classification of iron region in brain is presented in this paper. The local patch-based approach is combined with the feature extraction techniques to determine the powerful features from the given image. The patch-based features give 96.25% classification accuracy with robust classifier like random forest classifier.

The results of experiments conducted shows that the performance accuracy of classification obtained by implementing the proposed features is high compared to other state of art classification techniques. In order to achieve results of high quality, several issues have been addressed. We also describe the method in which we search for optimal values for parameters of RF classifier namely estimator and depth which is crucial for achieving best results. Future enhancement will be focused on implementation of efficient texture-based features on a larger image dataset.

References

- Araujo Salomao, R.P., Luiz Pedroso, J., Drumond Gama, M.T., Dutra, L.A., Maciel, R.H., Godeiro-Junior, C., Chien, H.F., Teive, H.A.G., Cardoso, F. and Barsottini, O.G.P. (2016) 'A diagnostic approach for neurodegeneration with brain iron accumulation: clinical features, genetics and brain imaging', *Arq Neuropsiquiatr*, Vol. 74, No. 7, pp.587–596.
- Batista-Nascimento, L., Pimentel, C., Andrade Menezes, R. and Rodrigues-Pousada, C. (2012) 'Iron and neurodegeneration: from cellular homeostasis to disease', *Oxidative Medicine and Cellular Longevity*, Vol. 2012, No. 1, pp.1–8.
- Bosch, A., Zisserman, A. and Munoz, X. (2007) 'Image classification using random forests and ferns', *2007 IEEE 11th International Conference on Computer Vision*, IEEE Xplore.

- Bustomi, M.A., Faricha, A., Ramdhan, A. and Faridawati (2018) 'Integrated image processing analysis and naive Bayes classifier method for lungs X-ray image classification', *ARPN J. Eng. Appl. Sci.*, Vol. 13, No. 2, pp.718–724.
- Gregory, A.M. and Hayflick, S.J. (2004) 'Neurodegeneration with brain iron accumulation', *Orphanet Encyclopedia*, Orphanet, France.
- Haacke, E.M., Mittal, S., Wu, Z., Neelavalli, J. and Cheng, Y-C.N. (2009) 'Susceptibility-weighted imaging: technical aspects and clinical applications, part 1', *AJNR Am J Neuroradiol.*, Vol. 30, No. 1, pp.19–30.
- Haacke, E.M., Xu, Y., Cheng, Y-C.N. and Reichenbach, J.R. (2004) 'Susceptibility weighted imaging (SWI)', *Magnetic Resonance in Medicine*, Vol. 52, No. 3, pp.612–618.
- Haralick, R.M., Shanmugam, K. and Dinstein, I. (1993) 'Textural features for image classification', *IEEE Transactions on Systems, Man and Cybernetics*, Vol. 3, No. 6, pp.610–621, SMC.
- Horning, N. (2010) 'Random forests: an algorithm for image classification and generation of continuous fields data sets', *International Conference on Geoinformatics for Spatial Infrastructure Development in Earth and Allied Sciences*.
- Hossein Sadrzadeh, S.M. and Saffari, Y. (2004) 'MD iron and brain disorders', *Am. J. Clin. Pathol.*, Vol. 121, Suppl. 1, No. 1, pp.S64–S70.
- Kotsiantis, S.B., Zaharakis, I.D. and Pintelas, P.E. (2006) 'Machine learning: a review of classification and combining techniques', *Artif. Intell. Rev.*, Vol. 26, No. 3, pp.159–190, Springer.
- Kruer, M.C. (2013) 'The neuropathology of neurodegeneration with brain iron accumulation', *Int. Rev. Neurobiol.*, Vol. 110, No. 1, pp.165–194.
- Kruer, M.C. and Boddaert, N. (2012) 'Neurodegeneration with brain iron accumulation: a diagnostic algorithm', *Semin Pediatr Neurol.*, Vol. 19, No. 2, pp.67–74.
- Kruer, M.C., Boddaert, N., Schneider, S.A., Houlden, H., Bhatia, K.P., Gregory, A., Anderson, J.C., Rooney, W.D., Hogarth, P. and Hayflick, S.J. (2012) 'Neuroimaging features of neurodegeneration with brain iron accumulation', *AJNR Am. J. Neuroradiol.*, Vol. 33, No. 3, pp.407–414.
- Lanciego, J.L., Luquin, N. and Obeso, J.A. (2012) *Functional Neuroanatomy of the Basal Ganglia*, Cold Spring Harb. Perspect. Med., Cold Spring Harbor Laboratory Press, USA.
- Murthy, S.K. (1998) 'Automatic construction of decision trees from data: a multi-disciplinary survey', *Data Mining and Knowledge Discovery*, Vol. 2, No. 24, pp.345–389.
- Oasis Brains Datasets [online] <http://www.oasis-brains.org> (accessed 20 February 2020).
- Ohta, E. and Takiyama, Y. (2012) 'MRI findings in neuroferritinopathy', *Neurology Research International*, Vol. 2012, No. 1, pp.1–7.
- Perez Ortiz, M., Jimenez Fernández, S., Gutierrez, P.A., Alexandre, E., Hervas Martinez, C. and Salcedo Sanz, S. (2016) 'A review of classification problems and algorithms in renewable energy applications', *Energies*, Vol. 9, No. 8, p.607.
- Schipper, H.M. (2012) 'Neurodegeneration with brain iron accumulation – clinical syndromes and neuroimaging', *Biochimica et Biophysica Acta*, Vol. 1822, No. 3, pp.350–360.
- Sheelakumari, R., Kesavadas, C., Varghese, T., Sreedharan, R.M., Thomas, B., Verghese, J. and Mathuranath, P.S. (2017) 'Assessment of iron deposition in the brain in frontotemporal dementia and its correlation with behavioral traits', *AJNR Am. J. Neuroradiol.*, Vol. 38, No. 10, pp.1953–1958.
- Stankiewicz, J., Panter, S.S., Neema, M., Arora, A., Batt, C. and Bakshi, R. (2007) 'Iron in chronic brain disorders: imaging and neurotherapeutic implications', *Neurotherapeutics*, Vol. 4, No. 3, pp.371–386.
- Thomas, L.O., Boyko, O.B., Anthony, D.C. and Burger, P.C. (1993) 'MR detection of brain iron', *AJNR*, Vol. 14, No. 5, pp.1043–1048.
- Udayabhanu, P., Viswan, A. and Padmarajan, S. (2016) 'MRI brain image classification using GLCM feature extraction and probabilistic neural networks', *International Conference on Emerging Trends in Engineering & Management (ICETEM-2016)*.
- Valdes Hernandez, M.d.C., Ritchie, S., Glatz, A., Allerhand, M., Munoz Maniega, S., Gow, A.J., Royle, N.A., Bastin, M.E., Starr, J.M., Deary, I.J. and Wardlaw, J.M. (2015) 'Brain iron deposits and lifespan cognitive ability', *AGE*, Vol. 37, No. 5, p.100, Springer, Dordr.
- Vijay, V., Kavitha, A.R. and Roselene Rebecca, S. (2016) *Procedia Computer Science*, Vol. 92, No. 1, pp.475–480, Elsevier, Netherlands (NL).
- Wilson, B. and Dhas, J.P.M. (2016) 'Evaluation of iron content in SWI brain images based on GLCM features', *IJCTA*, Vol. 9, No. 6, pp.33–40.
- Yan, S-Q., Sun, J-Z., Yan, Y-Q., Wang, H. and Lou, M. (2012) 'Evaluation of brain iron content based on magnetic resonance imaging (MRI): comparison among phase value, R2* and magnitude signal intensity', *PLoS ONE*, Vol. 7, No. 2, pp.1–6.
- Zacharakia, E.I., Wanga, S., Chawlaa, S., Yooa, D.S., Wolfa, R., Melhema, E.R. and Davatzikosa, C. (2009) 'Classification of brain tumor type and grade using MRI texture and shape in a machine learning scheme', *Magn. Reson. Med.*, Vol. 62, No. 6, pp.1609–1618.
- Zhang, Y., Dong, Z., Phillips, P., Wang, S., Ji, Yang, J. and Yuan, T-F. (2015) 'Detection of subjects and brain regions related to Alzheimer's disease using 3D MRI scans based on Eigen brain and machine learning', *Frontiers in Computational Neuroscience*, Vol. 9, pp.1–15, Article 66.